Analyst

PAPER

View Article Online
View Journal | View Issue

Cite this: *Analyst*, 2017, **142**, 925

Photochemistry in a soft-glass single-ring hollow-core photonic crystal fibre

Ana M. Cubillas,[a,b] Xin Jiang,*[a] Tijmen G. Euser,[a,c] Nicola Taccardi,[b,d] Bastian J. M. Etzold,[b,d,e] Peter Wasserscheid[b,d] and Philip St. J. Russell[a,b,f]

Received 22nd September 2016,
Accepted 5th January 2017

DOI: 10.1039/c6an02144a

rsc.li/analyst

A hollow-core photonic crystal fibre (HC-PCF), guided by photonic bandgap effects or anti-resonant reflection, offers strong light confinement and long photochemical interaction lengths in a microscale channel filled with a solvent of refractive index lower than that of glass (usually fused silica). These unique advantages have motivated its recent use as a highly efficient and versatile microreactor for liquid-phase photochemistry and catalysis. In this work, we use a single-ring HC-PCF made from a high-index soft glass, thus enabling photochemical experiments in higher index solvents. The optimized light–matter interaction in the fibre is used to strongly enhance the reaction rate in a proof-of-principle photolysis reaction in toluene.

Introduction

Photochemistry—the study of light-driven chemical reactions—plays an important role in nature, *e.g.*, in photosynthesis and, at the same time, has found a wide range of applications in industry, technology, and medicine.[1] Typically, high pump intensities are required to initiate and enhance photochemical reactions. We have recently shown that hollow-core photonic crystal fibres (HC-PCFs) can act as highly efficient microreactors for such studies.[2,3] HC-PCF consists of a central hollow-core of diameter ~20 μm, surrounded by a cladding formed by an array of hollow channels running along the entire length of the fibre.[4] Light is confined to the central hollow core either by a photonic bandgap[4] or by anti-resonant reflection (ARR) in fibres with kagomé-style[5] or single-ring[6–10] cladding structures. The use of single-ring ARR structures significantly reduces fabrication difficulties. In such fibres the central hollow core is surrounded by a ring of capillaries with a wall thickness from several hundred nm to a few μm. These capillaries act as off-resonance Fabry–Pérot (FP) resonators that frustrate leakage of light from the core, resulting in low loss-guidance.[6] Note that narrow high loss-bands appear at wavelengths where the core mode phase-matches the resonances in the thin glass walls, resulting in minima in fibre transmission. By appropriate design these resonances can be engineered to lie far away from the experimental wavelengths.

Recent studies have shown that, by careful design, higher order modes can be strongly suppressed in single-ring ARR HC-PCFs by a phase-matched coupling between higher-order core modes and leaky resonances in the surrounding capillaries.[8–11]

An important feature of HC-PCF is that its excellent guidance properties are preserved even when both core and cladding channels are filled with liquid, provided that the liquid index n_L is less than the index of the glass n_G.[12,13] The use of a liquid-filled ARR HC-PCF for photochemical experiments therefore effectively enables single-mode light guidance over meter-long path lengths, allowing a much higher sensitivity than in the case of conventional cuvette-based methods.[14] Importantly, the sample volume in the resulting optofluidic microreactors can be as small as a few nL per cm interaction length, while strong optical confinement in the core maximizes its interaction with the sample.[2] Finally, liquid and gaseous samples can be easily introduced into the hollow channels without the cumbersome post-processing techniques typically needed in conventional fibre-based chemical sensors.[15] These unique features have motivated the use of various types of PCF as chemical sensors[16] and, more recently, as efficient microreactors for photochemistry and catalysis.[3,17]

To date, these experiments have only been performed in fused silica HC-PCFs,[3] which limits the choice of solvent to liquids with a refractive index less than that of silica (n_G = 1.45

[a]*Max-Planck Institute for the Science of Light, Staudtstr 2, 91058 Erlangen, Germany. E-mail: xin.jiang@mpl.mpg.de*
[b]*Excellence Cluster "Engineering of Advanced Materials", University of Erlangen-Nuremberg, 91058 Erlangen, Germany*
[c]*NanoPhotonics Centre, Cavendish Laboratory, University of Cambridge, J. J. Thomson Avenue, Cambridge CB3 0HE, UK*
[d]*Lehrstuhl für Chemische Reaktionstechnik, University of Erlangen-Nuremberg, 91058 Erlangen, Germany*
[e]*Technische Universität Darmstadt, Ernst-Berl-Institut für Technische und Makromolekulare Chemie, 64287 Darmstadt, Germany*
[f]*Department of Physics, University of Erlangen-Nuremberg, 91058 Erlangen, Germany*

at 600 nm), if the benefits of single-mode guidance are to be preserved. This is because the guidance mechanism switches to total internal reflection (TIR) for $n_L > n_G$, resulting in an increasingly multi-mode operation as n_L rises, making accurate spectroscopic measurements very difficult.

In this paper we overcome the refractive index limitation of fused silica by using a single-ring ARR HC-PCF made from a lead-silicate glass (Schott SF6) with index n_G = 1.80 at 600 nm. The fibre was fabricated using an improved "stack-and-draw" technique.[18] The wavelength shift in the transmission spectrum of the fibre upon filling with a high-index solvent such as toluene (index n_L = 1.49 at 600 nm) is measured. In a proof-of-principle experiment, we use this fibre to demonstrate the photochemical conversion of an organometallic complex in toluene.

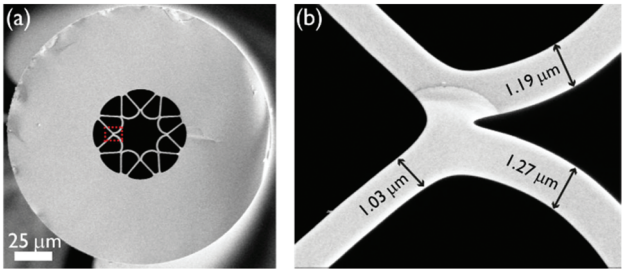

Fig. 2 Scanning electron micrographs (SEMs) of (a) the soft-glass single-ring ARR HC-PCF and (b) a close-up of a portion of the surrounding glass membranes. The fibre has a core diameter of ~25 μm, and an average core wall thickness of 1.2 μm. The design reduces confinement loss by anti-resonant reflection between the core mode and modes of the surrounding single-ring.[8]

Methods and experimental

Fabrication of soft-glass single-ring hollow-core PCFs

Currently, single-ring ARR HC-PCFs are mainly made from fused silica glass.[6–10] The use of high-index soft glasses as fibre materials for PCFs is much more challenging because of a much faster change in viscosity with temperature as well as glass devitrification during heating. Consequently, the drawing conditions must be precisely controlled within a narrow temperature range (±5 to ±25 °C)[18–20]—much narrower than for fused silica (±150 °C)—and often an inert atmosphere is necessary. Reports of HC-PCFs being fabricated from lead-silicate and chalcogenide glasses can only be found in recent papers.[18,20] Using improved fabrication procedures, we drew single-ring ARR HC-PCFs from soft-glass for this study. In contrast to the kagomé HC-PCFs used in previous photochemistry experiments,[2] the simpler single-ring structure significantly reduces the sample infiltration time, due to the wider hollow channels in the cladding ring.

The Schott SF6 lead-silicate glass used has a drawing temperature of ~610 ± 10 °C, corresponding to a glass viscosity ranging from $10^{5.5}$ to $10^{5.9}$ Pa s. The stacking procedure is depicted in Fig. 1. Eight capillaries of diameter 670 μm were drawn (Fig. 1, left), stacked in a full circle (Fig. 1, middle) and inserted together into a jacket tube (Fig. 1, right). The stack was supported by a central tube/rod inserted at each end, and the structure was drawn down to a cane with sub-mm scale features. In the final fibre drawing step, the pressures in the core and surrounding small capillary holes were independently controlled so as to produce the desired structure. The drawn fibre has a core of diameter 25 μm (Fig. 2a) surrounded by capillaries with wall thickness ~1.2 μm (Fig. 2b).

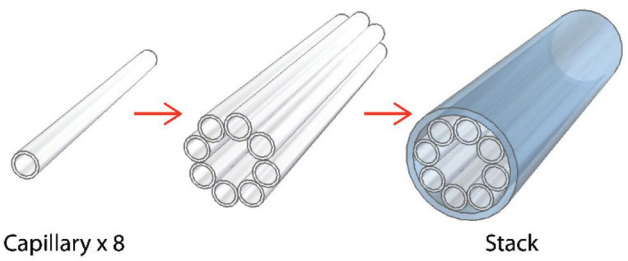

Fig. 1 Schematic illustration of the stacking procedure used to form the single-ring HC-PCF structure. More details on the "stack-and-draw" technique can be found in previous publications.[4]

Fibre characterization

The transmission spectrum of the single-ring ARR HC-PCF was recorded using an optical spectrum analyser (Yokogawa AQ6315E), and a home-built, silica PCF-based supercontinuum (SC) source, emitting from 500 to 1900 nm. For the photochemical experiments, a compact 405 nm laser diode (LD) was used both as the excitation source and probe (Thorlabs, LDM405, 0.5 mW emitted power). A power meter was used to monitor changes in the absorption. By spatially filtering the laser diode output using an endlessly single-mode PCF with core diameter 8 μm, launch efficiencies of typically 30% into the single-ring HC-PCF could be achieved.

The transmission spectrum of an air-filled 25 cm-long ARR HC-PCF is shown in Fig. 3a (solid blue curve). Undistorted single-lobed fundamental modes were observed for each transmission window (Fig. 3b). The wavelengths of minimum transmission correspond to resonances in the glass membranes in the cladding, following the relationship:[6]

$$\lambda_m = \frac{2d}{m}\sqrt{{n_G}^2 - {n_{01}}^2} \approx \frac{2d}{m}\sqrt{{n_G}^2 - {n_L}^2} \quad (1)$$

where n_{01} is the index of the LP_{01}-like core mode, d is the thickness of the glass membranes surrounding the core and m is the order of resonance. The observed transmission dips (solid blue curve in Fig. 3a) are in reasonable agreement with the resonant wavelengths calculated using eqn (1), which coincide with the loss peaks (dashed red curve) calculated for a hollow-core capillary with the same core diameter and a wall thickness equal to that of the membranes in the drawn fibre. The presence of the thick silica sheath will tend to pull the wall indices to higher values which, together with higher-order modes that create field lobes parallel to the membranes, will broaden and shift the resonant peaks to longer wavelengths, as seen in Fig. 3.

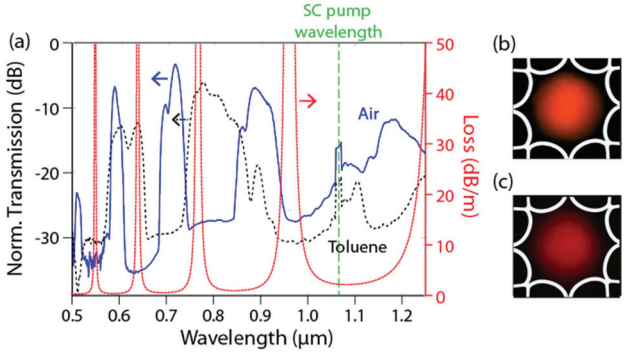

Fig. 3 (a) Normalized transmission in air-filled (solid blue) and toluene-filled (dashed black) soft-glass single-ring ARR HC-PCFs. The loss spectrum for an air-filled fibre (dashed red) is calculated analytically, assuming a capillary waveguide with the same core diameter and wall thickness. Note that the low-loss windows (red) are consistent with the measured high-transmission bands (blue). The peaks at ~1.064 μm in the measured transmission spectra are from the pump laser of the supercontinuum source. (b) & (c) Measured near-field mode profiles in the (b) air-filled and (c) toluene-filled single-ring ARR HC-PCFs.

Next, all the hollow channels were filled with toluene (n_L = 1.49), resulting in a blue-shift of the spectral features (dashed black curve), as predicted by eqn (1). Due to the higher index of the Schott SF6 glass, broadband single-mode guidance could be achieved for both air and toluene (Fig. 3b and c), making this simplified soft-glass single-ring ARR HC-PCF an excellent candidate for photochemical reactions in higher-index liquids.

Photochemical microreactor

The set-up used for photochemical experiments is shown in Fig. 4a, and closely resembles previous experiments.[2,3] The ends of the soft-glass ARR HC-PCF were placed into two custom-built liquid cells (Fig. 4b) and microscope objectives were used to free-space couple light into and out of the fibre. A beam-splitter was used to reflect a small fraction of the light transmitted through the HC-PCF onto a camera, so as to measure the intensity profile of the guided mode (Fig. 4b and c). The remaining light was measured by using a detector. The liquid sample was delivered *via* a syringe pump (KD Scientific, KDS 410) containing the reactant dissolved in toluene. Note that the fibre used in the photochemical experiment is similar to the one shown in Fig. 1, but with glass membranes roughly half as thick (~600 nm) for better transmission properties in the UV. A scanning electron micrograph (SEM) of the structure is shown in Fig. 4c. The result was a much better guidance at 405 nm in the toluene-filled fibre. The transmission loss of the fibre when filled with pure toluene was 38 dB m^{-1} at 405 nm, caused predominantly by confinement and scattering losses in toluene but also by absorption losses. The overall insertion and transmission loss was 13 dB along the 35 cm-long ARR HC-PCF.

Principle

The reaction used for proof-of-principle was a light-induced intermolecular C–H bond activation of the organometallic complex $(HBPz'_3)Rh(CO)_2$ (Pz′ = 3,5-dimethylpyrazolyl) dissolved in toluene.[21] As demonstrated in ref. 21 the absorption spectrum of the un-irradiated $(HBPz'_3)Rh(CO)_2$ complex features a broad absorption peak that is centred around the excitation wavelength λ_{ex} = 356 nm, with a peak molar absorptivity of 2100 M^{-1} cm^{-1}. While these data were measured in *n*-pentane, the absorption features in this range are attributed to the ligand field states and are therefore expected to exhibit negligible solvent sensitivity.[21] Upon irradiation with visible light, the following CO dissociation reaction takes place:[21]

$$(HBPz'_3)Rh(CO)_2 \xrightarrow[\text{toluene},C_7H_8]{h\nu} (HBPz'_3)Rh(CO)(C_7H_7)H + CO$$

The absorbance peak at λ_{ex} = 356 nm is not present in the right-hand photoproduct, resulting in a light-induced decrease in

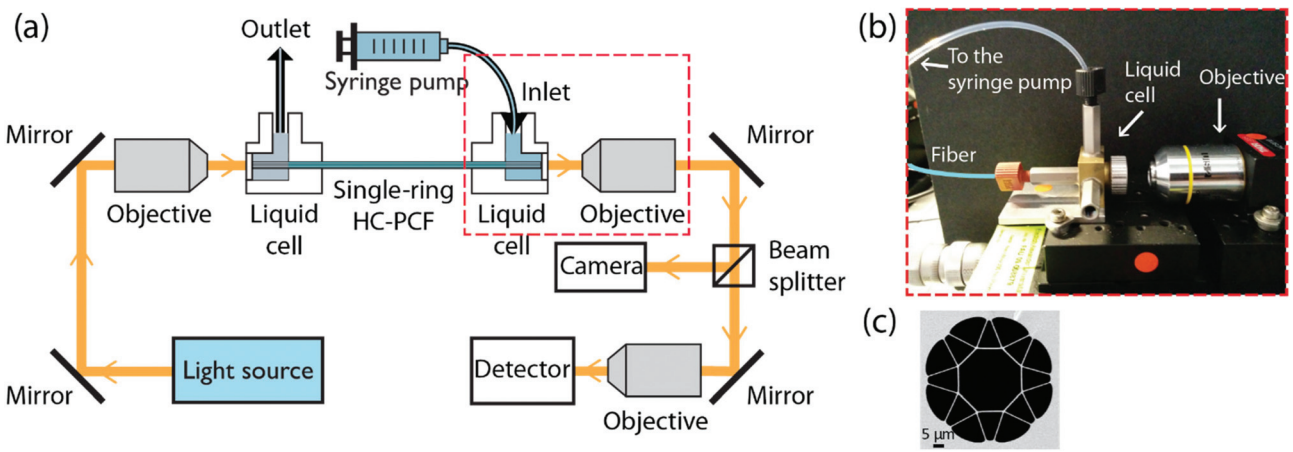

Fig. 4 (a) Set-up used for the photochemical experiments. A 35 cm-long SF6 glass single-ring ARR HC-PCF is used. Two custom-built liquid cells were used for filling the toluene solvent into the fibre. Laser-light is coupled to the fibre using an (under-filled) 4× 0.1 NA objective, and the output is imaged onto a CCD camera and a detector. (b) An image of the sample filling system (liquid cell, fibre and light incoupling), shown within the dotted rectangle in (a). (c) SEM of the fibre used for the photochemical experiments: wall thickness ~600 nm, 30 μm core diameter.

Table 1 (Upper) Experimental parameters and fitted values for the quantum yield in the photochemical experiments in toluene in the fibre. (Lower) Quantum yield values obtained in ref. 21

λ_{ex} [nm]	P [μW]	Coupling efficiency	ϕ
405	30.0	33%	0.0051
405	15.0	20%	0.0053
405	11.1	33%	0.0031
405	5.2	32%	0.0029
From ref. 21			
366	—	—	0.14
458	—	—	0.0073

absorbance. The reaction is characterized by a low quantum yield, *i.e.*, the number of dissociation events per photon absorbed is very low ($\phi \sim 0.0073$ at 458 nm (ref. 21)) in the visible wavelength range. This reaction will therefore strongly benefit from the enhanced light–matter interaction in the ARR HC-PCF.

Experimentally, a 35 cm-long length of the ARR HC-PCF was filled with a 10 μm solution of $(HBPz'_3)Rh(CO)_2$ in toluene. The total sample volume was less than 175 nL, representing a 10 000-fold reduction compared to a 1 cm cuvette-based measurement. At the same time, the 35 times longer path length in the fibre results in a higher detection sensitivity. The reaction was driven by pumping the shoulder of the 356 nm absorption band with a diode laser running at λ_{ex} = 405 nm. The molar absorptivity of the un-irradiated compound at this wavelength was measured to be ~1000 M^{-1} cm^{-1} using a conventional UV-Vis spectrometer (Shimadzu UV-300). The excitation powers used in the experiment were between 5 and 30 μW (before launching into the fibre). The measured coupling efficiency for each experiment is shown in Table 1, with typical values around 30%. The reaction was monitored by measuring the power in the transmitted excitation light with a photodiode.

Results and discussion

The resulting relative absorbance decay (with $A(t)$ the absorbance at time t and $A(0)$ the initial absorbance) for different input powers is plotted in Fig. 5 (data-points). As expected, a clear decrease in absorption was observed over time, the reaction rate depending on the excitation power. As a reference, the photolysis experiment was also performed in a 1 cm quartz cuvette containing 3 ml volume with C = 100 μM. The cuvette was irradiated with 420 μW of blue light using the same diode laser. Remarkably, despite almost a two orders of magnitude higher input power in the cuvette, the reaction took more than 8 hours to complete (asterisks in Fig. 5), highlighting the enhanced light–matter interaction provided by the ARR HC-PCF.

The measured reaction dynamics were compared to a mathematical model of the system, in which the quantum yield ϕ was treated as a single, freely adjustable parameter. The model takes into account the loss-induced 13 dB intensity drop along the fibre, which results in a position-dependent reaction rate. A more detailed description of the model is available elsewhere,[2] where it was applied to aqueous photolysis experiments in silica-glass HC-PCFs. The quantum yield was fitted for each experiment, and the curves obtained are in good agreement with the data (Fig. 5). The values obtained for ϕ lie between 0.003 and 0.005, in close agreement with published data[21] at nearby excitation wavelengths (Table 1).

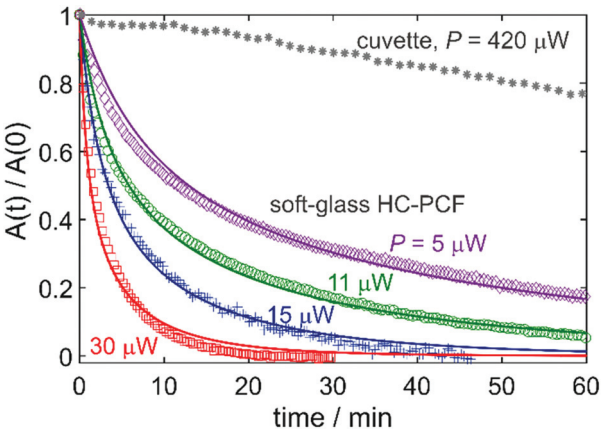

Fig. 5 (Symbols) Measured absorbance decay of a sample with an initial concentration C = 10 μM of $(HBPz'_3)Rh(CO)_2$ in toluene, in a 35 cm-long soft-glass single-ring ARR HC-PCF. The colors correspond to different input powers. The grey data points correspond to a reference measurement in a 1 cm-long cuvette with C = 100 μM. The solid curves correspond to a mathematical model of the system (the values obtained for the quantum yield are summarized in Table 1).

Conclusions

In summary, a single-ring ARR HC-PCF made from a high-index glass allows the single-mode guidance of light in high-index liquids, permitting well-controlled studies of photochemical reactions in high-index solvents. The much enhanced light intensity in the hollow fibre core of a single-ring ARR HC-PCF microreactor (compared to cuvettes) greatly accelerates the photochemical processes, making it possible to monitor chemical reactions with very small quantum yields, such as the photolysis of organometallic complexes in toluene. The results open up a wide range of possibilities for studying photochemical reactions in sub-μL samples in high-index organic solvents.[22]

Acknowledgements

The authors would like to acknowledge the contributions from F. Babic, G. Ahmed and J. Potschka for assisting the work in various ways.

References

1 K. Rohatgi-Mukherjee, in *Fundamentals of photochemistry*, New Age International, 1978.

2 J. S. Y. Chen, T. G. Euser, N. J. Farrer, P. J. Sadler, M. Scharrer and P. St. J. Russell, *Chem. – Eur. J.*, 2010, **16**, 5607–5612.
3 A. M. Cubillas, S. Unterkofler, T. G. Euser, B. J. M. Etzold, A. C. Jones, P. J. Sadler, P. Wasserscheid and P. St. J. Russell, *Chem. Soc. Rev.*, 2013, **42**, 8629–8648.
4 P. St. J. Russell, *Science*, 2003, **299**, 358–362.
5 F. Benabid, J. C. Knight, G. Antonopoulos and P. St. J. Russell, *Science*, 2003, **298**, 399–402.
6 N. M. Litchinitser, A. K. Abeeluck, C. Headley and B. Eggleton, *Opt. Lett.*, 2002, **27**, 1592–1594.
7 A. D. Pryamikov, A. Biriukov, S. A. F. Kosolapov, V. G. Plotnichenko, S. L. Semjonov and E. M. Dianov, *Opt. Express*, 2011, **19**, 1441–1448.
8 F. Yu, W. J. Wadsworth and J. C. Knight, *Opt. Express*, 2012, **20**, 11153–11158.
9 P. Uebel, M. C. Gunendi, M. H. Frosz, G. Ahmed, N. N. Edavalath, J.-M. Menard and P. St. J. Russell, *Opt. Lett.*, 2014, **41**, 1961–1964.
10 A. Hartung, J. Kobelke, A. Schwuchow, J. Bierlich, J. Popp, M. A. Schmidt and T. Frosch, *Opt. Lett.*, 2015, **40**, 8429–8436.
11 C. Wei, C. R. Menyuk and J. Hu, *Opt. Express*, 2016, **24**, 12228–12239.
12 T. A. Birks, D. M. Bird, T. D. Hedley, J. M. Pottage and P. St. J. Russell, *Opt. Express*, 2004, **12**, 69–74.
13 F. M. Cox, A. Argyros and M. C. J. Large, *Opt. Express*, 2006, **14**, 4135–4140.
14 A. M. Cubillas, M. Schmidt, M. Scharrer, T. G. Euser, B. J. M. Etzold, N. Taccardi, P. Wasserscheid and P. St. J. Russell, *Chem. – Eur. J.*, 2012, **18**, 1586–1590.
15 J. M. López-Higuera, in *Handbook of optical fibre sensing technology*, John Wiley & Sons Ltd, Chichester, England, 2002.
16 A. M. R. Pinto and M. Lopez-Amo, *J. Sens.*, 2012, 598178.
17 M. Schmidt, A. M. Cubillas, N. Taccardi, T. G. Euser, T. Cremer, F. Maier, H.-P. Steinrück, P. St. J. Russell, P. Wasserscheid and B. J. M. Etzold, *ChemCatChem*, 2013, **5**, 641–650.
18 X. Jiang, T. G. Euser, A. Abdolvand, F. Babic, F. Tani, N. Y. Joly, J. C. Travers and P. St. J. Russell, *Opt. Express*, 2011, **19**, 15438–15444.
19 X. Jiang, N. Y. Joly, M. A. Finger, F. Babic, G. K. L. Wong, J. C. Travers and P. St. J. Russell, *Nat. Photonics*, 2015, **9**, 133–139.
20 A. F. Kosolapov, A. D. Pryamikov, A. S. Biriukov, V. S. Shiryaev, M. S. Astapovich, G. E. Snopatin, V. G. Plotnichenko, M. F. Churbanov and E. M. Dianov, *Opt. Express*, 2011, **19**, 25723–25728.
21 A. A. Purwoko, S. D. Tibensky and A. J. Lees, *Inorg. Chem.*, 1996, **35**, 7049–7055.
22 C. Reichardt and T. Welton, in *Solvents and solvent effects in organic chemistry*, John Wiley & Sons, 2011.